Links between climate and sea levels for the past three million years

Kurt Lambeck*†, Tezer M. Esat* & Emma-Kate Potter*

**Research School of Earth Sciences, Australian National University, Canberra 0200, Australia*
†Swedish Research Council and Lund University, Tornavägen 13, S223 63, Sweden

The oscillations between glacial and interglacial climate conditions over the past three million years have been characterized by a transfer of immense amounts of water between two of its largest reservoirs on Earth — the ice sheets and the oceans. Since the latest of these oscillations, the Last Glacial Maximum (between about 30,000 and 19,000 years ago), ~50 million cubic kilometres of ice has melted from the land-based ice sheets, raising global sea level by ~130 metres. Such rapid changes in sea level are part of a complex pattern of interactions between the atmosphere, oceans, ice sheets and solid earth, all of which have different response timescales. The trigger for the sea-level fluctuations most probably lies with changes in insolation, caused by astronomical forcing, but internal feedback cycles complicate the simple model of causes and effects.

The onset of Pleistocene glaciations occurred about three million years ago with formation of permanent ice sheets at high northern latitudes. As the ice sheets waxed and waned, the concomitant fall and rise of sea level left direct evidence for the intensity and timing of glacial cycles. The major sea-level cycles occur at intervals of ~100,000 years (100 kyr) over the past ~800 kyr, with maximum amplitudes of 120–140 m, involving changes in ice volume of 50–60 million km^3. Superimposed on these are lesser cycles of a few tens of thousands of years and shorter duration.

Direct, accurate and high-resolution observations of past sea levels exist only for the last glacial cycle, from about 130 kyr ago to the present. Knowledge of ice volume for the earlier periods rests increasingly on proxy indicators contained within oozes of calcareous skeletons of marine foraminifera shells. These record the isotopic and chemical signatures of the water in which they lived, and the ratio of two oxygen isotopes $^{18}O/^{16}O$ is particularly important. It is the lighter isotope that is preferentially evaporated, whereas during precipitation the heavier isotope condenses preferentially. Thus, as water vapour is transported poleward this ratio shifts to lesser values and is reflected in the isotopic signature of high-latitude snow. At times of major glaciations, the oceans become depleted in the lighter oxygen isotope.

The isotope ratio $\delta^{18}O = \{(^{18}O/^{16}O)_{sample}/(^{18}O/^{16}O)_{standard} - 1\}$, expressed as parts per thousand, is therefore believed to be an indicator of global ice volume — low values indicate small ice volumes and hence globally warm conditions, and high values imply large ice sheets and low temperatures[1,2]. In foraminifera, this ratio is also a function of local seawater temperature and independent observations become important for establishing not only the links between the sea-level fluctuations and climate, but also for calibrating the proxy indicators. Accumulating evidence reveals a complex pattern of change throughout Pleistocene time, particularly for the last glacial cycle, with a variable role for astronomical forcing and an interaction between oceans, atmosphere, ice and solid earth that is rich in its implications for climate change.

Onset of glacial cycles in sea level

Records of foraminifera have been preserved in open-ocean marine sediments from two localities over the past 5 million years (Myr)[3,4] (Fig. 1). The record before ~3 Myr is

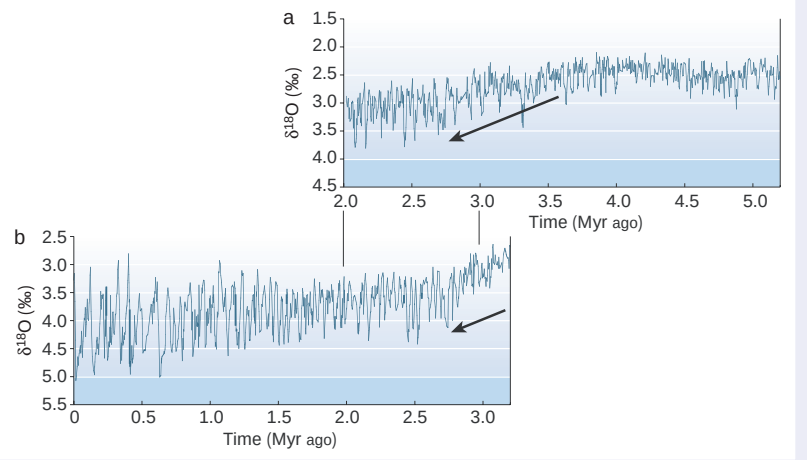

Figure 1 $\delta^{18}O$ records for the past 5 Myr from two sediment cores. **a**, Site 999 in the Caribbean Sea[4]; **b**, Site ODP-607 from the equatorial Atlantic[3]. For the early part of the record (before ~3.2 Myr ago) the average $\delta^{18}O$ is low and the oscillations are of relatively small amplitude. This is indicative of globally warm conditions without major ice sheets in the Northern Hemisphere. At ~2.7 Myr ago both the oscillations and the mean value are larger, with a principal periodicity of ~40 kyr. After ~0.8 Myr ago the major oscillation occurs with a periodicity of ~100 kyr.

characterized by low $\delta^{18}O$ and the early period is one of relatively high global temperatures with little ice locked up in polar caps. After ~3 Myr the oscillations become larger and indicate onset of glaciation in the Northern Hemisphere, with successive glaciations becoming progressively more intense. This onset coincides with a marked increase in lithic material in high-latitude North Atlantic sediment cores[4,5] carried by the first calving of Northern Hemisphere ice into the Atlantic. At ~0.8 Myr ago the pattern of $\delta^{18}O$ oscillations shifts from the principal periodicity of 40 kyr to 100 kyr (ref. 6). The 100-kyr pattern becomes established in the sea-level record during this interval[7–10].

Growth of large ice sheets requires warm temperatures during winters to enhance moisture transport to high latitudes, and cool temperatures during summers to prevent melting of snow. Surface water transports heat efficiently and a northward penetration of warm surface currents can encourage ice-sheet development, while suppression of these currents discourages ice growth. Thus changes in climate, ocean circulation and ice-sheet growth and decay are closely linked[11–14]. A number of factors can modify this circulation. Changes in tectonic configuration of the continents can drive warm surface currents towards or away from high latitudes. The closure of the Isthmus of Panama may have been important in this context, because as the waterway between the two Americas narrowed, warm surface Atlantic currents were probably deflected northwards. The timing of the final stages of closure between about 3.6 and 2.7 Myr ago[4,15] is sufficiently close to the onset of Northern Hemispheric glaciation to make an attractive hypothesis: that the tectonically driven change in the Atlantic circulation leads to increased moisture transport to high latitudes and to the development of the northern ice sheets. Once established, the ice sheets can increase the supply of cold water to the oceans, which feeds back into the surface currents. Superimposed upon this tectonic–ocean–ice interaction will be any external forcing of the climate.

Under the influence of gravitational interactions between the Earth, Sun and Moon, the insolation at the upper atmosphere varies cyclically[16] and the same periodicities are observed in the $\delta^{18}O$ records[17]. Known as the Milankovitch forcing, this indicates that astronomical forces exert a strong ordering influence on climate[16,18,19], although some significant differences do exist. For example, the climate periodicity of 100 kyr is only weakly present in orbital frequencies, and a strong 413-kyr cycle seen in insolation predictions is not reflected in climate variability[20]. On a timescale of a few million years the orbital and rotational motions in the Solar System are stable[21], and if astronomical forcing is the only agent for change then the same climate behaviour is expected throughout, in contrast to the fundamental changes seen at ~3 and ~0.8 Myr ago. Thus, processes and feedbacks other than astronomical motions are likely to be important in influencing climate variability[11,13,20]. Suggestions for feedback modes are many, but satisfactory solutions are few. Where there is agreement is that changes in ocean circulation, whose response to external forcing contains both short (~1 kyr) and longer (3–5 kyr) time constants, can modify climate response to external forcing and feedback mechanisms[22,23].

Numerous explanations have been advanced for the dominant 100-kyr cycle in the climate record. Most involve the long response times associated with massive ice sheets[24,25], others involve forcing by orbital inclination[26]. However, atmospheric variables extracted from the Vostok ice core and from marine cores follow a 100-kyr cycle in phase with astronomical forcing, indicating that this cycle is not related to ice-sheet dynamics[27]. Instead, it seems to be a response (with appropriate time lag) to forcing by air temperature. This leaves unanswered the cause of the temperature forcing and why it started only ~0.8 Myr ago. But, it means that the relationship between $\delta^{18}O$ and sea-level fluctuations is more complex than sometimes assumed, reinforcing the need to establish an independent sea-level record free of proxy indicators. Availability of increasingly accurate observations of past sea-level positions should lead to answers to some of the questions raised by the proxy records and hence to an improved understanding of the processes that have driven climate change in the past.

Earlier glacial cycles and sea level

Observational records of sea level consist of positions and ages of remnants of former shorelines. Coral reefs[9,10,28] and speleothems (reprecipitated carbonates)[29] provide a chronology of mainly interglacial periods and these confirm the recurrence of the ~100-kyr cycle. The amplitudes of sea-level change during the early interglacials are poorly known because many of the locations where records are preserved are also subject to tectonic uplift. Thus it remains impossible to say with certainty whether there was more or less ice globally than today during any of the past interglacials and whether the behaviour of the Greenland and West Antarctic ice sheets differs from interglacial to interglacial. The observed timing of earlier interglacials, at ~630 kyr ago[10], ~330 kyr ago[10,30] and ~200 kyr ago[29], is consistent with the hypothesis of astronomically forcing. But, other than for the last interglacial, it has not yet been possible to define with precision the timing of the onset and termination of these periods or to establish in detail the phase relationship(s) between Milankovitch forcing, sea level and oxygen isotope signals for the same interval. Current evidence suggests that the last two interglacials were of approximately equal length (~12 kyr)[29,31].

Sedimentological evidence has provided some estimate of sea levels during the major glacials preceding the interglacials[32–34], and global ice volumes during successive glacial maxima seem to have been of similar magnitude to that of the Last Glacial Maximum (LGM; see below). One possible exception is at ~ 450 kyr ago, when ice volumes may have been some 15% greater than during the last glaciation[32], and greater than at any other time in the past 3 Myr. Determining where this ice was will remain uncertain until a coherent chronology for the terrestrial record of the early glaciations is established.

The last glacial cycle

In areas of tectonic uplift, sea-level markers have occasionally been elevated beyond the reach of the destructive forces of succeeding cycles. However, because the quality of the exposed record often deteriorates as a result of weathering, a quasi-continuous sea-level record is still only available for the last glacial cycle, from about 130 kyr ago to the present. This reveals a much finer structure than do the older fragments, one that is diagnostic of higher-frequency interactions between climate, ocean and ice.

Coral reefs form particularly good records. Coral growth proliferates when the rate of sea-level rise equals or exceeds the rate of land uplift, but when sea-level rise cannot keep up only patchy and thin reef veneers develop. Important examples are from Barbados[35], Sumba[9] and Papua New Guinea[8,36,37]. Uplift at Huon Peninsula, Papua New Guinea, is as high as 4 mm yr^{-1}, resulting in a more detailed record than is available from other localities. Huon terraces of last interglacial age are now at elevations up to 400 m, whereas in tectonically stable areas such reefs occur near modern sea level[31]. Comparison between the two sites yields estimates for the rate of tectonic uplift, while evidence from the latter sites is used to establish the timing of the interval when ice volume was last near its present volume[28,31]. Information from river delta sequences at Huon constrains the sea-level position of intervening lowstands[34]. Uranium-series dating of the corals[38,39] completes the process, leading to a relation between age, sea level and height[40] (Fig. 2). Although the Huon data have already received considerable attention, new high-resolution results are providing fresh insights into the behaviour of ice sheets, thermohaline circulation and sea level[41,42].

The last glacial cycle is divided into marine oxygen isotope stages (MIS) 1–5 based on distinct patterns of fluctuation in $\delta^{18}O$ in marine sediments[43]. MIS-5 includes the last interglacial (substage MIS-5e) and a series of oscillations between increasingly cold stadials and relatively warm interstadials (substages 5d–5a; Fig. 2). MIS-4 and -3

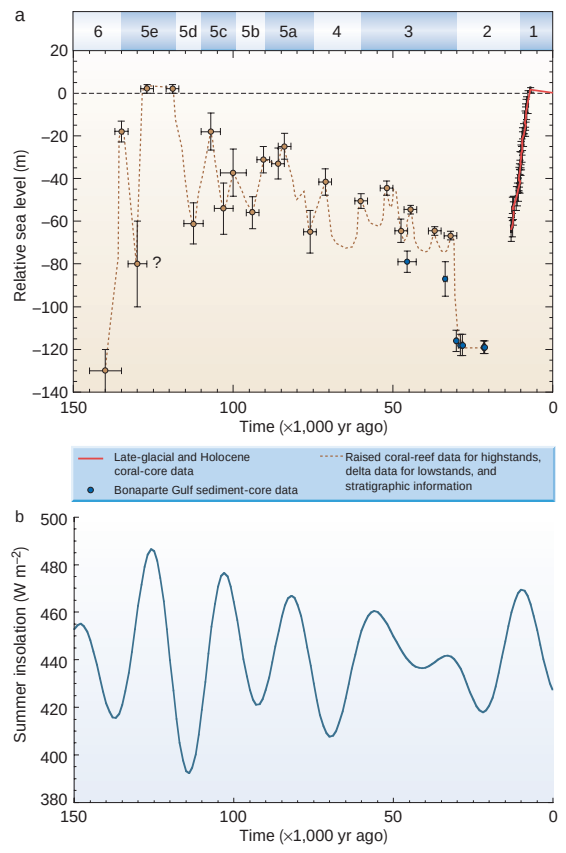

Figure 2 Relative sea level and insolation for the last glacial cycle. **a**, The relative sea-level curve for the last glacial cycle for Huon Peninsula[40] supplemented with observations from Bonaparte Gulf, Australia[73]. Error bars define the upper and lower limits. The timescale is based on uranium-series ages of corals older than about 30 kyr (refs 36–38) and on calibrated radiocarbon ages of the younger corals and sediments (all U-Th ages here and in Fig. 3 have been subjected to strict evaluation criteria[31]). The main oxygen isotope stages MIS-5 to MIS-1, including the substages of MIS-5, are identified. The results represent conservative estimates, with each oscillation identified being supported by several precisely dated points from one or more reef section, by the stratigraphic relationship of the sampled corals to the reef crest position, and by models of reef growth in an environment of changing sea levels[42]. The local minima in sea level during MIS-5 are based on the positions of stream deltas relative to the reefs defining local highstands[34]. These lowstands have not been dated, but their positions are consistent with modelling results of reef growth[42]. Although it is not normally permissible to combine sea-level data from different localities without first correcting for differential isostatic effects, in this particular case the Huon and Bonaparte locations are at continental margins far from former ice loads and the differences in isostatic corrections are less than the uncertainties in the data[75]. Thus the Bonaparte data are assumed to be valid for Huon within the error bars indicated. **b**, Insolation curve for July at 65° N.

correspond to the period leading into the maximum glaciation and represents a time of stadials, of increasing intensity, punctuated by brief interstadials. MIS-2 includes the LGM followed by a period of rapid ice decay. The past ~12,000 years defines MIS-1 or the Holocene, when ice volumes and climate were largely similar to those of today.

Into and out of the last interglacial period

The end of the last interglacial (MIS-5e) marks a return to glacial conditions at high northern latitudes and, along with substages 5d to 5a, forms a possible analogue for the termination of the Holocene. Shorelines and coral reefs formed during MIS-5e are a few metres higher than modern sea level and the highest levels may have occurred midway through the period[31]. These higher values cannot be related directly to differences in ice volume between this period and the Holocene because of the isostatic adjustment of the Earth in response to ice-water loads before and after reef formation[44,45]. What can be concluded is that it is unlikely that there were major differences in ice volume (<2–4 m in equivalent sea level) between the two interglacials.

Sea levels during the last interglacial reached present values for the first time around 130 kyr ago[31,46]. However, if the analogy with the Holocene is valid, interglacial temperatures in mid-latitudes will have been attained as much as 6,000 years before the sea approached its modern level, and this is indeed supported by terrestrial $\delta^{18}O$ records[47] and other marine deposits[48]. The period leading out of the penultimate glacial maximum and into the last interglacial remains poorly constrained. Sea levels during this maximum were about the same as during the LGM[33,34], but the timing is not established quantitatively. The subsequent sea-level rise seems to have been rapid, possibly with a swift, large-amplitude oscillation before modern levels were reached[37,46].

At Huon and Barbados, well-developed monolithic reef structures formed during the major interstadials MIS-5a and MIS-5c[8,35] when global sea levels were 20–30 m lower than today. Relative highstands corresponding to MIS-5a have also been recorded in Florida[49,50] and Bermuda[49], but their elevations are affected by isostatic adjustment to past ice loads more than at Barbados and Huon. After differential isostatic corrections are applied, the results are consistent within the uncertainties of the observations and the model corrections[45]. During the stadials MIS-5b and MIS-5d, sea levels have been as much as 40–60 m below present levels[40]. For comparison, the Scandinavian and Laurentian ice sheets at maximum limits contained enough ice to lower sea level by ~12–15 m and ~60–80 m, respectively[51]. Thus, substantial ice sheets existed during the MIS-5 stadials.

Few pre-LGM ice margins and shorelines have been preserved that provide even approximate constraints on thickness or location of earlier glaciations and, where they have been identified, there is debate about their age. In Scandinavia, MIS-5d is recognized as a cool period during which ice was restricted to the high ground of Norway and Sweden[52,53], contributing only a few metres to the change in global sea level. The glaciation during stage MIS-5b was more extensive, but still only a small fraction of its subsequent maximum volume. Only by MIS-4 did a large ice sheet form over Scandinavia. In between these stadials, the ice retreated to the mountains or disappeared entirely[54]. Instead, the major Eurasian glaciation began over Arctic Russia with a large ice sheet over the Kara Sea and western Siberia[55]. Field estimates of ice margins during stages 5b and 4, including observations of ice overriding the higher mountains of the region[55], indicate a glaciation comparable in size to the LGM Scandinavian ice. When ice grew over Scandinavia during MIS-4, to the east it started to retreat and by the coldest time (MIS-2) the Kara Sea shelves and Arctic Russia were largely free of glacier ice[55]. Likewise, in North America the early MIS-5 glaciations initiated in Arctic Canada and successive glaciations advanced progressively southwards during MIS-5d to -4 while decaying in the north[56].

The mechanisms by which the Eurasian and North American ice sheets developed following MIS-5e remain uncertain and speculative. However, the early growth of ice sheets at high latitudes indicates an enhanced moisture supply to the Arctic regions compared to the present, possibly because during warmer parts of the last interglacial, permanent Arctic sea-ice cover was less extensive than during subsequent periods. This introduces moisture into the polar areas and enables snow to accumulate without requiring a significant lowering of temperature. As falling global temperatures initiate ice build-up in Scandinavia, the sea ice returns and a precipitation shadow develops that starves the eastern region of further snow. A similar scenario could be envisaged for North America. Open sea conditions at high latitudes during the late stages of the last interglacial allow ice to

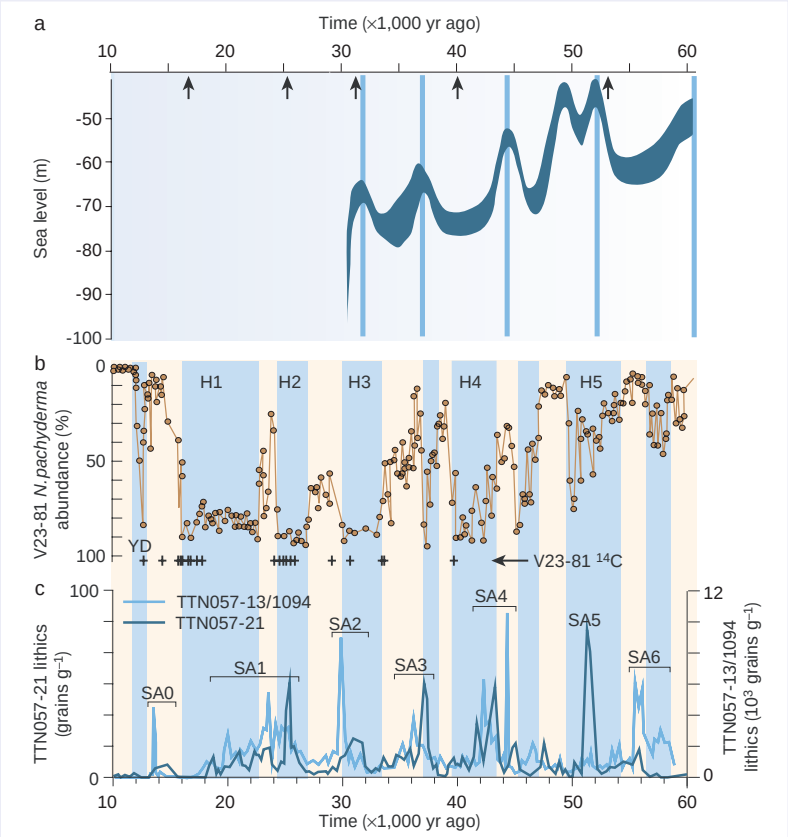

Figure 3 Comparison of MIS-3 sea-level oscillations and Atlantic sediment records. **a**, Sea-level curve for MIS-3 coral terraces from Huon Peninsula, Papua New Guinea. Upper and lower bounds are shown. **b**, *Neogloboquadrina pachyderma* (s.) abundances from the North Atlantic core V23-81[59] plotted on the same calendar timescale. The original radiocarbon ages[57,59] from the depths in the core marked by (+) have been converted to calendar ages. The extent of major Heinrich events identified in the North Atlantic cores, corresponding to cold periods, are within the colour bands. The arrows identify the mean timing of Heinrich events[62]. **c**, IRD from two South Atlantic cores TTN057-21 and TTN057-13/1094 (ref. 60). Within the uncertainties of the calendar age determinations, the South Atlantic IRD peaks correspond to the cold events in the North Atlantic.

develop initially over Arctic Canada. The subsequent cooling, and the southern march of the North American ice sheet, leads to a precipitation shadow causing the northern ice to decay at the same time as the maximum southern limit is reached. Thus it is tempting to suggest that onset of a glacial cycle after a prolonged interglacial requires the break up of Arctic sea ice and enhanced exposure of Arctic air to relatively warm surface water. The accumulation of snow and ice increases albedo at high latitudes, which then feeds back into the global climate system. A test of this hypothesis would be to demonstrate that temperature during the MIS-5 fluctuations lags the fall in sea-level.

Leading into the maximum glaciation

Sea level after MIS-5 did not fall uniformly towards its LGM level, but oscillated rapidly with amplitudes of 10–15 m about every 4,000 years (the approximate duration of a half cycle[36,41]; Fig. 2). There is a clear visual distinction between the MIS-3 and MIS-5 reefs at Huon, the former being less developed, more numerous and possessing more complex sub-structures, a distinction that is mirrored in the $\delta^{18}O$ records. The implication is that fluctuations in climate and its ice-volume response were more rapid during MIS-3 than during MIS-5.

Five highstands have been identified within the MIS-3 interval, centred on 32, 36, 44, 49–52 and 60 kyr ago (Fig. 3). Periods of high abundance of the planktonic foraminiferan *Neogloboquadrina pachyderma* sinistral (left-coiling) in the North Atlantic core V23-81 closely match the $\delta^{18}O$ variations and correspond to cold water temperatures[57]. These periods also coincide with episodes of ice-rafted debris (IRD) deposits in both the North[58,59] and South Atlantic (for example, peaks SA0 to SA6)[60] (Fig. 3). Variations in IRD abundances in the two hemispheres are in agreement except for the additional peak at about 37 kyr ago in the South Atlantic record. There is, however, a sharp enhancement in *N. pachyderma* abundance in core V23-81, indicating that this southern IRD event occurs within a cold interval in the Northern Hemisphere. Periods of cooler upper-ocean temperature and increased IRD define Heinrich events (H1 to H6)[58,61] of which the last four occurred during MIS-3 (ref. 62; and see review in this issue by Rahmstorf, pages 207–214).

Heinrich events are attributed to instabilities in the ice sheets once they have grown to continental dimensions, resulting in iceberg discharge. The increased supply of fresh cold water, from melting icebergs at high-latitudes in the North Atlantic, is believed sufficient to dilute the warm, saline surface waters and prevent them from sinking[63,64]. The consequential slow-down or interruption in the thermohaline circulation causes a cold snap, reduction in freshwater supply to the ocean and the eventual re-establishment of North Atlantic Deep Water formation[65]. The cycle is completed over the next several thousand years when renewed moisture supply and snow precipitation leads to re-growth of the ice sheets.

The chronology of the sedimentary records after ~50 kyr ago is usually related to the radiocarbon timescale, whereas corals are usually dated using uranium-series methods. Radiocarbon ages become increasingly uncertain with age, not only because of their decreasing levels of ^{14}C, but also because ^{14}C production in the atmosphere varies with time. In particular, anomalous rates of ^{14}C production and large excursions from a uniform timescale occur during Heinrich events[41,66,67]. Uranium-series ages, although more accurate than radiocarbon ages for this time interval, may also not be as accurate as formal precision estimates suggest because of the possibility of coral diagenesis[28,31].

Although accurate phase relations between sediment records and sea-level oscillations cannot yet be established, the following three conclusions can at least be drawn from a comparison of the sediment and coral results[41]. First, periods of enhanced reef development recorded by the Huon terraces correlate with cold intervals; second,

reef growth occurs in response to rising sea level caused by ice-sheet collapse during cold periods; and third, ice discharge at times of Heinrich events raises global sea level by 10–15 m. If these conclusions are accepted then the best definition of the timing of Heinrich events is established not by the uncertain ^{14}C chronology, but by the Huon uranium-series reef ages.

The amplitude of sea-level rise represents 15–25% of Laurentide ice volume or the total volume of Scandinavian LGM ice. Thus the Heinrich events are associated with significant and rapid changes in the ice sheets. Different locations have been identified for the source regions of IRD. Some of the thickest and most rapidly deposited layers are close to the Hudson Strait, and the Laurentide ice sheet is a chief source[68]. But deposits of similar timing originate from the European ice sheet[69] and the correspondence between South and North Atlantic deposits suggests that coeval fluctuations in ice volume occur in Antarctica[70]. Thus there must be strong and swift interactions between the major ice sheets in both hemispheres, in which the collapse of one ice sheet raises sea level sufficiently to destabilize those margins of the others where ice advanced onto the shelves[71]. According to this scenario, rapid sea-level rises need not be sought in the collapse of only a single ice sheet.

The Last Glacial Maximum

The lowest sea levels at any time during the last glacial cycle occurred from ~30 kyr ago to ~19 kyr ago[72]; this period constitutes the LGM when land-based ice volumes were ~55×10^6 km^3 greater than present[73,74]. Onset of the LGM was rapid, with sea level falling ~30–40 m within 1,000–2,000 years[75]. The growth in ice is consistent with evidence from Scandinavia that extensive ice-free conditions ended before ~30 kyr ago[76] with rapid expansion of ice from Norway and Sweden over the North Sea[77] and Finland[78]. Similar ice-sheet expansion is required in North America or Antarctica to explain the observed magnitude of sea-level change. The rapidity of sea-level lowering events, including those recorded during MIS-3 Heinrich cycles, indicate that ice sheets can expand quickly under favourable conditions of moisture supply.

Observations of local sea level at and within the former ice margins provide constraints on the contributions of individual ice sheets to the total ice volume[79,80]. During glacial loading, the crust beneath the ice is depressed and rebounds slowly when ice is removed, at a rate determined by the earth's rheology and by the ice-load history. By exploiting the spatial and temporal variability of the sea-level response, some separation of earth and ice parameters can be achieved. Near the former centre of glaciation, the contribution of the crustal rebound dominates sea-level change and results in a characteristic exponentially decreasing function. For sites near but within the maximum ice margin, the rebound and global-rise signals are of comparable magnitude but opposite in sign, producing the typical ice-margin signal from Vesterålen, Norway (Fig. 4a). Here organic sediments indicate that the offshore islands were partly ice free as early as 21.5 kyr ago when local sea level stood 35 m higher than today[81]. If the LGM ice never extended beyond this location, the predicted levels are considerably lower than observed because the rebound is insufficient to overcome the rise from the added global meltwater. Only if the ice stood at the shelf edge, ~50 km offshore and ~1,000–1,500 m thick, do predicted levels begin to match the observed values[80].

A similar conclusion is drawn from age–height observations of shorelines on Baffin Island, Canada. In some reconstructions of the North American ice sheet, the maximum ice margin does not reach the coast during the LGM; rather the ice limit remains near the heads of the fiords[82]. Sea-level curves are similar to those observed along the Norway coast (Fig. 4b), but if ice reached only the upper fiord regions the predicted values are mostly below sea level. Only if ice extended onto the shelf do predictions agree with observed evidence. A recent re-evaluation of geomorphological evidence, supplemented with cosmogenic age data, concludes that the ice did indeed extend offshore in the south, but not in the north[83]. Sea-level analyses for Svalbard[84], Greenland[85] and East Antarctica[86] lead to similar conclusions that, at the height of glaciation, the ice sheets extended offshore, in most cases as far as the shelf margin where they were susceptible to rapid reductions in volume.

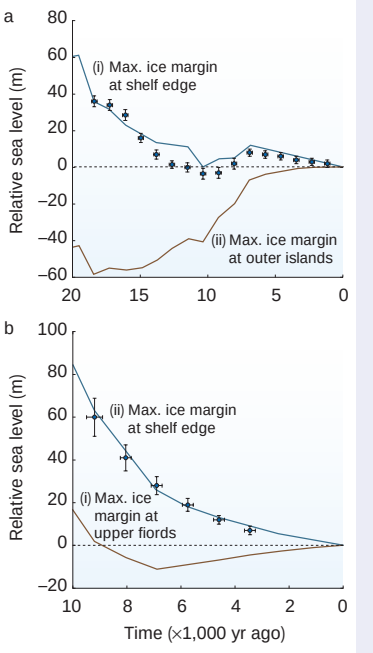

Figure 4 Sea-level fluctuations near former ice margins. **a**, Data from Andøya, Vesterålen, northern Norway. The observed evidence[81] is shown by the circles with error bars. Predicted values[80] are shown for two ice models: (i) where the maximum ice margin is located at the continental edge at the time of the LGM and before the site became ice free; and (ii) where the maximum ice margin extended only to the present coast. **b**, Data from Baffin Island, Canada. The observed sea levels[79] are shown by the open circles. The model predictions are for: (i) an ice model in which the ice did not expand beyond the upper fiords of eastern Baffin Island[81]; and (ii) a model in which the ice margin has been shifted 80 km eastwards and onto the shelf, retaining the same height profile as in (i). Only in the latter case is there good agreement between observations and predictions. The expansion of the ice onto the shelf is consistent with the re-interpretation of morphological evidence[83] from southern and central Baffin Island. It is not consistent, however, with evidence from northern Baffin Island where the few available sea-level indicators also imply thick LGM ice cover onto the adjacent shelf, but the morphological re-interpretation is that the ice cover was more restricted[83]. We suspect that further re-interpretation of the field data will be necessary before this discrepancy is resolved.

The thickness of the ice can be constrained by the amplitudes of local sea level. The rebound predicted for the steeply domed CLIMAP ice model[87] is greater than observed for a wide range of plausible mantle rheologies, indicating that the ice thickness is overestimated[79,80]. But if the volumes of the individual ice sheets are scaled down uniformly such that predicted and observed rebound agrees, then the total ice volumes become inadequate to explain the observed LGM sea levels. However, the mostly late- and post-glacial rebound data do not adequately constrain ice volumes at the LGM and the observations are also consistent with rebound models in which ice sheets that were initially steeply domed experienced early rapid reduction[88]. The observed rapid sea-level rise of about 10–15 m after 19 kyr ago[73] coincides with a substantial IRD influx, mainly of Scandinavian origin, into the Irminger Basin[89], which suggests that a major change occurred in the Scandinavian ice sheet at this time. Alternatively (or additionally), this sea-level rise could have an Antarctic origin, as the $\delta^{18}O$ signal from the Southern Ocean[90] and the Antarctic Vostok ice core[91] indicates that warming in the Southern Hemisphere started abruptly at about 20 kyr ago and that a partial dispersal of the grounded shelf ice followed soon after.

The late- and post-glacial period

The post-LGM record from localities far from the ice sheets indicates that sea-level rise was not temporally uniform (Fig. 5). On some shallow continental shelves, such as within the Persian Gulf, now-submerged shorelines developed that are indicative of constant sea level,

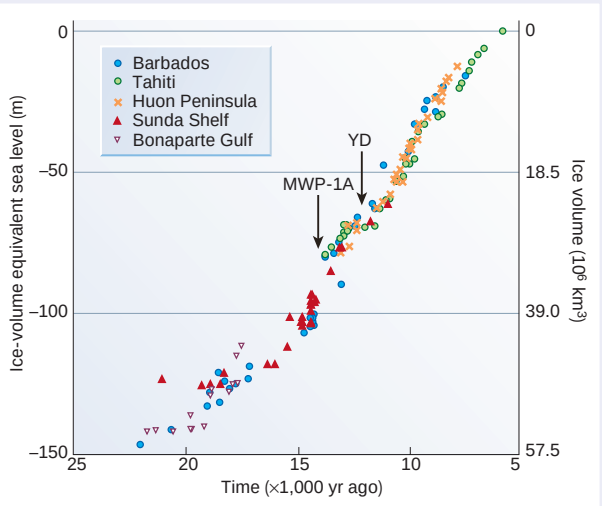

Figure 5 Changes in global ice volume from the time of the LGM to the present. The figure shows ice-volume equivalent sea level for the past 20 kyr based on isostatically adjusted sea-level data from different localities[73,93–96]. Because of spatial variability of the sea-level response to the glacial and water loading, sea-level observations from different localities should not be combined into a single sea-level curve unless the isostatic effects can be shown to be similar. The ice-volume equivalent sea-level function used here corresponds to the observed sea levels corrected for these effects[75]. It relates to the change in total ice volume, with respect to the present, of continent-based ice and any ice grounded on the shelves. With one exception, the results indicate an ice volume at the LGM that was ~55×10^6 km^3 greater than at present[74,75]. The error bars, not shown, are typically 0.1–0.15 kyr in calendar years and 5 m or less in position. MWP-1A refers to the timing of the meltwater pulse at ~14 kyr ago. At the Younger Dryas (YD) at ~12 kyr ago, sea-level rise may have momentarily halted.

particularly about the time of the Younger Dryas[92]. This is also seen in Fig. 5 as a short-duration period at ~12 kyr ago when ice volumes remained constant. A period of sustained global melting occurred from ~19–7 kyr ago, but periods of more rapid rise can also be identified within this interval[93]. A gap in the Barbados record occurs at ~14 kyr ago, at a time when sea level rose at a rate of about 40 mm yr^{-1} (ref. 94).

The record is not well defined for this latter period, possibly because of a sampling artefact or because the coral growth could not keep pace with the rapid sea-level rise, but a similar hiatus has been identified in the coral record from Tahiti[95]. Furthermore, data from the Sahul Shelf[96], which are free from 'keep-up' considerations, support a rapid rise of about ~15 m between 16–14 kyr ago, although data of greater temporal resolution are again desirable. This meltwater pulse, MWP-1A[94], reflects a rapid decay of ice sheets, but no consensus on the source has been reached, with contributions from North America, Scandinavia and the Barents Sea, and Antarctica having been proposed[97,98]. Estimates vary for the timing of H1 — the major post-LGM episode of IRD deposition in the North Atlantic — but most terminate this event before or at the time of MWP-1A[58,62] and the relationship between the two events remains unclear. MWP-1A is followed by the Younger Dryas stadial during which the thermohaline circulation did slow down and large-scale cooling occurred, but not to the same extent as occurred during the MIS-3 events. It is possible that the astronomical forcing of climate was now sufficiently influential to disrupt the earlier high-frequency cyclic behaviour and, as for the early part of the glacial cycle, was able to exert its dominating influence on climate.

More questions than answers

During the Pleistocene epoch of Earth history, glaciations have dominated and interglacials occurred for less than 10% of the time. The current interglacial interval has persisted for about as long as the duration of earlier interglacials and a return to stadial conditions should not be unanticipated if the past is any guide to the future; sea-level and climate fluctuations during the last interglacial may well provide an interesting analogue for an eventual termination of the present interglacial.

The causes of the climate fluctuations that repeatedly built up and destroyed ice sheets remain unclear. Sea-level fluctuations during the last glacial cycle have responded to the dominant oscillations in insolation, with periodicities of ~40 kyr and ~20 kyr (Fig. 2). But the relative amplitudes and phase relationships show no consistent match. The onset of the maximum in sea level preceded the peak in Northern Hemisphere summer insolation in the last interglacial[31,44,47,48], whereas for the present interglacial the insolation peak preceded the sea-level maximum. The insolation minima at ~140 and ~20 kyr ago correspond to the two associated glacial maxima, but at ~115 kyr ago, for example, insolation was even lower, without a correspondingly lower value in sea level.

The timing of the penultimate glacial maximum has not yet been adequately constrained by quantitative chronological data, but the rise in sea level seems to start at about the time of the solar minimum. Likewise, the end of the LGM coincides with an insolation minimum. The stadials MIS-5d and -5b, and possibly MIS-4, also occur at the time of minima in insolation. This is perhaps the most consistent correlation between the two functions throughout this cycle.

The lack of an overall correlation may be related to the influence on climate of other parameters, in addition to the summer insolation at 65° N. For example, a higher-latitude insolation index may be more appropriate or, more significantly, Southern Hemisphere insolation may also be important, and Antarctic ice may respond independent of Northern Hemisphere changes or with a time lag[62]. Various attempts at defining an insolation index that leads to a more clear-cut correlation have so far proved unsuccessful[99,100].

The structure of the sea-level curve shows greater high-frequency fluctuations than does the insolation index. This sea-level evidence, along with other proxy indicators of climate, points to a multitude of interrelated forces and feedbacks that are more important at some periods than others (see also the commentary in this issue by Kump, pages 188–190). It seems that during the early part of the glacial cycle, insolation controls the glacial oscillations and sea level but, starting at about MIS-4, feedback mechanisms become increasingly important. By the time ice sheets have become long-term features of the Northern Hemisphere landscape, reaching the continental shelves and becoming unstable, the subtle interplay between Milankovitch cycles, ice-sheet dynamics and shifts in ocean circulation seems to drive the climate system. At ~20 kyr ago, and possibly during the penultimate glacial maximum, the oscillations in insolation once again take over and break the higher-frequency feedback cycle. Insolation now dominates, notwithstanding brief oscillations back into ice-age conditions caused by the feedback processes, as evidenced by a rapid sea-level oscillation during the transition from MIS-6 to MIS-5[37] and the short-lived, stationary sea level during the Younger Dryas cold period[64]. □

doi:10.1038/nature01089

1. Mix, A. C. & Ruddiman, W. F. Oxygen isotope analyses and Pleistocene ice volumes. *Quat. Res.* **21,** 1–20 (1984).
2. Shackleton, N. J. Oxygen isotope analyses and Pleistocene temperatures re-assessed. *Nature* **215,** 15–17 (1967).
3. Raymo, M. E. in *Start of a Glacial* (eds Kukla, G. J. & Went, E.) 207–223 (Springer, Berlin, 1992).
4. Haug, G. H. & Tiedeman, R. Effect of the formation of the Isthmus of Panama on Atlantic Ocean thermohaline circulation. *Nature* **393,** 673–676 (1998).
5. Shackleton, N. J. Oxygen isotope calibration of the onset of ice-rafting and history of glaciation in the North Atlantic region. *Nature* **307,** 620–623 (1984).
6. Shackleton, N. J. & Opdyke, N. D. Oxygen isotope and palaeomagnetic stratigraphy of equatorial Pacific core V28-238: oxygen isotope temperatures and ice volumes on a 10^5 year scale and 10^6 year scale. *Quat. Res.* **3,** 39–55 (1973).
7. Broecker, W. S. & van Donk, J. Insolation changes, ice volumes and the ^{18}O record in deep-sea cores. *Rev. Geophys. Space Phys.* **8,** 169–198 (1970).
8. Chappell, J. Geology of coral terraces, Huon Peninsula, New Guinea: a study of Quaternary tectonic

movements and sea-level changes. *Bull. Geol. Soc. Am.* **85,** 553–570 (1974).
9. Pirazolli, P. A. *et al.* Quaternary raised coral-reef terraces on Sumba Island, Indonesia. *Science* **252,** 1834–1836 (1991).
10. Stirling, C. H. *et al.* Orbital forcing of the marine isotope stage 9 interglacial. *Science* **291,** 290–293 (2001).
11. Broecker, W. S. & Denton, G. H. The role of ocean-atmosphere reorganizations in glacial cycles. *Geochim. Cosmochim. Acta* **53,** 2465–2501(1989).
12. McManus, J. F., Oppo, D. W. & Cullen, J. L. A 0.5-million-year record of millennial-scale climate variability in the North Atlantic. *Science* **283,** 971–975 (1999).
13. MacAyeal, D. R. Binge/purge oscillations of the Laurentide ice sheets as a cause of the North Atlantic's Heinrich events. *Paleoceanography* **8,** 775–784 (1993).
14. Alley, R. B. & Clark, P. U. The deglaciation of the northern hemisphere: a global perspective. *Annu. Rev. Earth Planet. Sci.* **27,** 149–182 (1999).
15. Hay, W. W. The cause of the Late Cenozoic Northern Hemisphere glaciations: a climate change enigma. *Terra Nova* **4,** 305–311 (1992).
16. Berger, A. Milankovitch theory and climate. *Rev. Geophys.* **26,** 624–657 (1988).
17. Emiliani, C. Pleistocene temperatures. *J. Geol.* **63,** 538–578 (1955).
18. Hays, J. D., Imbrie, J. & Shackleton, N. J. Variations in the earth's orbit: pacemaker of the ice ages. *Science* **194,** 1121–1132 (1976).
19. Duplessy, J. C., Chenouard, L. & Villa, F. Weyl's theory of glaciation supported by isotopic study of Norwegian core K11. *Science* **188,** 1208–1209 (1975).
20. Imbrie, J. *et al.* On the structure and origin of major glaciation cycles, 2. The 100,000-year cycle. *Paleoceanography* **8,** 699–735 (1993).
21. Berger, A, Loutre, M. F. Lascar, J. Stability of the astronomical frequencies over the earth's history for paleoclimate studies. *Science* **255,** 560–566 (1992).
22. Imbrie, J. *et al.* On the structure and origin of major glaciation cycles, 1. Linear responses to Milankovitch forcing. *Paleoceanography* **7,** 701–738 (1992).
23. Imbrie, J., Berger, A. & Shackleton, N. J. in *Global Changes in the Perspective of the Past* (eds Eddy, J. A. & Oescher, H.) 263–277 (Wiley, Chichester, 1993).
24. Imbrie, J. & Imbrie, J. Z. Modelling the climatic responses to orbital variations. *Science* **207,** 943–953 (1980).
25. Clark, P. U. & Pollard, D. Origin of the middle Pleistocene transition by ice sheet erosion of regolith. *Paleoceanography* **13,** 1–9 (1998).
26. Muller, R. A. & MacDonald, G. J. F. Glacial cycles and astronomical forcing. *Science* **277,** 215–218 (1997).
27. Shackleton, N. J. The 100,000-year ice-age cycle identified and found to lag temperature, carbon dioxide, and orbital eccentricity. *Science* **289,** 1897–1902 (2000).
28. Gallup, C. D., Edwards, R. L. & Johnson, R. G. The timing of high sea levels over the past 200,000 years. *Science* **263,** 796–800 (1994).
29. Bard, E., Antonioli, F. & Silenzi, S. Duration and timing of the penultimate interglacial sea level highstand: implications for the astronomical theory of palaeoclimate. *Earth Planet. Sci. Lett.* **196,** 135–146 (2002).
30. Galewsky, J., Silver, E. A., Gallup, C. D., Edwards, R. L. & Potts, D. C., Foredeep tectonics and carbonate platform dynamics in the Huon Gulf, Papua New Guinea. *Geology* **24,** 819–822 (1996).
31. Stirling, C. H., Esat, T. M., Lambeck, K. & McCulloch, M. T. Timing and duration of the Last Interglacial: evidence for a restricted interval of widespread coral reef growth. *Earth Planet. Sci. Lett.* **160,** 745–762 (1998).
32. Rohling, E. J. *et al.* Magnitudes of the sea-level lowstands of the past 500,000 years. *Nature* **394,** 162–165 (1998).
33. Ferland, M. A., Roy, P. S. & Murray-Wallace, C. V. Glacial lowstand deposits on the outer continental shelf of southeastern Australia. *Quat. Res.* **44,** 294–299 (1995).
34. Chappell, J. & Shackleton, N. J. Oxygen isotopes and sea level. *Nature* **324,** 137–140 (1986).
35. Mesolella, K., Matthews, R. K., Broecker, W. S. & Thurber, D. L. The astronomical theory of climate change: Barbados data. *J. Geol.* **77,** 250–274 (1969).
36. Chappell, J. *et al.* Reconciliation of late Quaternary sea levels derived from coral terraces at Huon Peninsula with deep sea oxygen isotope records. *Earth Planet. Sci. Lett.* **141,** 227–236 (1996).
37. Esat, T. M., McCulloch, M. T., Chappell, J., Pillans, B. & Omura, A. Rapid fluctuations in sea level recorded at Huon Peninsula during the Penultimate Deglaciation. *Science* **283,** 197–201 (1999).
38. Yokoyama, Y., Esat, T. M., Lambeck, K. & Fifield, L. K. Last ice age millennial scale climate changes recorded in Huon Peninsula corals. *Radiocarbon* **42,** 383–401 (2000).
39. Stein, M. *et al.* TIMS U-series dating and stable isotopes of the last interglacial event in Papua New Guinea. *Geochim. Cosmochim. Acta* **57,** 2541–2554 (1993).
40. Lambeck, K. & Chappell, J. Sea level change through the last glacial cycle. *Science* **292,** 679–686 (2001).
41. Yokoyama, Y., Esat, T. M. & Lambeck, K. Coupled climate and sea-level changes deduced from Huon Peninsula coral terraces of the last ice age. *Earth Planet. Sci. Lett.* **193,** 579–587 (2001).
42. Chappell, J. C. Sea-level changes forced ice breakouts in the Last Glacial cycle: new results from coral terraces. *Quat. Sci. Rev.* **21,** 1229–1240 (2002).
43. Imbrie, J. *et al.* in *Milankovitch and Climate* (eds Berger, A. *et al.*) 269–305 (Reidel, Dordrecht, 1984).
44. Lambeck, K. & Nakada, M. Constraints on the age and duration of the last interglacial period and on sea-level variations. *Nature* **357,** 125–128 (1992).
45. Potter, E.-K. *et al.* Timing and magnitude of oxygen isotope stage 5a and 5c sea level oscillations at Barbados: implications for the melting history of the Laurentide ice sheet during OIS 5 and 6. *Eos Trans. AGU* **82**(47), Fall Meet. Suppl., Abstract PP12A-0467 (2001).
46. Gallup, C. D., Cheng, H., Taylor, F. W. & Edwards, R. L. Direct determination of the timing of sea level change during termination II. *Science* **295,** 310–313 (2002).
47. Winograd, I. J. *et al.* Continuous 500,000 year climate record from vein calcite in Devils Hole, Nevada. *Science* **258,** 255–260 (1992).
48. Henderson, G. M. & Slowey, N. C., Evidence from U-Th dating against northern hemisphere forcing of the penultimate deglaciation. *Nature* **404,** 61–65 (2000).
49. Ludwig, K. R. *et al.* Sea level records at ~80ka from tectonically stable platforms: Florida and Bermuda. *Geology* **24,** 211–214 (1996).
50. Toscano, M. A. & Lundberg, J. Submerged Late Pleistocene reefs on the tectonically-stable S.E. Florida margin: high-precision geochronology, stratigraphy, resolution of Substage 5a sea-level elevation, and orbital forcing. *Quat. Sci. Rev.* **18,** 753–767 (1999).
51. Denton, G. H. & Hughes, T. J. (eds) *The Last Great Ice Sheets* (Wiley, New York, 1980).
52. Lundqvist, J. in *Glacial Stratigraphy, Engineering Geology and Earth Construction* (ed. Kauranne, K.) (Geol. Surv. Finland Special Paper 15) 43–59 (Geol. Surv. Finland, 1992).
53. Helmens, K. F., Räsänen, M. E., Johansson, P. W., Jungner, H. & Korjonen, K. The last interglacial-glacial cycle in NE Scandinavia: a nearly continuous record from Sokli (Finnish Lapland). *Quat. Sci. Rev.* **19,** 1605–1623 (2000).
54. Mangerud, J. Ice sheet limits in Norway and on the Norwegian continental shelf. *Quat. Sci. Rev.* (submitted).
55. Svendsen, J. I. *et al.* Maximum extent of the Eurasian ice sheets in the Barents and Kara Sea region during the Weichselian. *Boreas* **28,** 234–242 (1999).
56. Clark, P. U. *et al.* Initiation and development of the Laurentide and Cordilleran ice sheets following the Last Interglaciation, *Quat. Sci. Rev.* **12,** 79–114 (1993).
57. Lund, D. C. & Mix, A. C. Millennial-scale deep water oscillations: reflections of the North Atlantic in the deep Pacific from 10 to 60 ka. *Paleoceanography* **13,** 10–19 (1998).
58. Bond, G. *et al.* Evidence for massive discharges of icebergs into the North Atlantic ocean during the last glacial period. *Nature* **360,** 245–249 (1992).
59. Bond, G. *et al.* Correlations between climate records from North Atlantic sediments and Greenland ice. *Nature* **365,**143–147 (1993).
60. Kanfoush, S. L. *et al.* Millennial-scale instability of the Antarctic ice sheet during the last glaciation, *Science* **288,** 1815–1818 (2000).
61. Heinrich, H. Origin and consequences of cyclic ice rafting in the northeast Atlantic Ocean during the last 130,000 years. *Quat. Res.* **29,** 143–152 (1988).
62. Chapman, M. R., Shackleton, N. J. & Duplessey, J.-C., Sea surface temperature variability during the last glacial-interglacial cycle assessing the magnitude and pattern of climate change in the North Atlantic. *Palaeogeogr. Palaeoclimatol. Palaeoecol.* **157,** 1–25 (2000).
63. Broecker, W. S. Massive iceberg discharges as triggers for global climate change. *Nature* **372,** 421–424 (1994).
64. Fawcett, P. J., Agustsdottir, A. M., Alley, R. B. & Shuman, C. A. The Younger Dryas termination and the North Atlantic deep water formation: insights from climate model simulations and Greenland ice cores. *Paleoceanography* **12,** 23–38 (1997).
65. Alley, R. B. Icing the North Atlantic. *Nature* **392,** 335–337 (1998).
66. Kitagawa, H. & van der Plicht, J., Atmospheric radiocarbon calibration to 45,000 yr B.P.: late glacial fluctuations and cosmogenic isotope production. *Science* **279,** 1187–1190 (1998).
67. Hughen, K. A., Southon, J. R., Lehman, S. J. & Overpeck, J. T. Synchronous radiocarbon and climate shifts during the last deglaciation. *Science* **290,** 1951–1954 (2000).
68. Broecker, W. S. & Hemming, S. Climate swings come into focus. *Science* **294,** 2308–2309 (2001).
69. Dowdeswell, J. A., Elverhøi, A., Andrews, J. T. & Hebbeln, D. Asynchronous deposition of ice-rafted layers in the Nordic seas and North Atlantic Ocean. *Nature* **400,** 348–351 (1999).
70. Shemesh, A., Burckle, L. H. & Hays, J. D. Meltwater input to the Southern Ocean during the Last Glacial Maximum. *Science* **266,** 1542–1544 (1994).
71. Bond, G. C. & Lotti, R. Iceberg discharges into the North Atlantic on millennial time scales during the Last Glaciation. *Science* **267,** 1005–1010 (1995).
72. Mix, A. C., Bard, E. & Schneider, R. Environmental processes of the ice age land, oceans, glaciers (EPILOG). *Quat. Sci. Rev.* **20,** 627–657 (2001).
73. Yokoyama, Y., Lambeck, K., De Deckker, P., Johnston, P. & Fifield, L. K. Timing of the Last Glacial Maximum from observed sea-level minima. *Nature* **406,** 713–716 (2000). [Published correction in *Nature*, **412**, 99 (2001).]
74. Milne, G. A., Mitrovica, J. X. & Schrag, D. P. Estimating past continental ice volume from sea-level data. *Quat. Sci. Rev.* **21,** 361–376 (2002).
75. Lambeck, K., Yokoyama, Y. & Purcell, A., Into and out of the Last Glacial Maximum: sea-level change during oxygen isotope stages 3 and 2. *Quat. Sci. Rev.* **21,** 343–360 (2002).
76. Olsen, L., Sveian, H. & Bergstrøm, B. Rapid adjustments of the western part of the Scandinavian ice sheet during the Mid and Late Weichselian—a new model. *Norw. J. Geol.* **81**, 93–118 (2001).
77. Sejrup, H. P. *et al.* Quaternary glaciations in southern Fennoscandia: evidence from southwestern Norway and the northern North Sea. *Quat. Sci. Rev.* **19,** 667–685 (2000).
78. Ukkonen, P., Lunkka, J. P., Jungner, H. & Donner, J. New radiocarbon dates from Finnish mammoths indicating large ice-free areas in Fennoscandia during the Middle Weichselian. *J. Quat. Sci.* **14,** 711–714 (1999).
79. Tushingham, A. M. & Peltier, W. R. ICE-3G: a new global model of Late Pleistocene deglaciation based upon geophysical predictions of postglacial sea-level change. *J. Geophys. Res.* **96,** 4497–4523 (1991).
80. Lambeck, K., Smither, C. & Johnston, P. Sea-level change, glacial rebound and mantle viscosity for northern Europe. *Geophys. J. Int.* **134,** 647–651 (1998).
81. Vorren, T. O., Vorren, K.-D., Alm, T., Gullimsen, S. & Løvlie, R. The last deglaciation (20,000–11,000 B.P.) on Andøya, northern Norway. *Boreas* **17,** 41–77 (1988).
82. Licciardi, J. M., Clark, P. U., Jenson, J. W. & MacAyeal, D. R. Deglaciation of a soft-bed Laurentide ice sheet. *Quat. Sci. Rev.* **17,** 427–448 (1998).
83. Miller, G. H. *et al.* The Goldilocks dilemma: big ice, little ice, or "just-right" ice in the Eastern Canadian Arctic. *Quat. Sci. Rev.* **21,** 33–48 (2002).
84. Lambeck, K. Limits on the areal extent of the Barents Sea ice sheet in Late Weichselian time. *Palaeogeogr. Palaeoclimatol. Palaeoecol.* **12,** 41–51 (1996).
85. Bennike, O., Björck, S. & Lambeck, K. Estimates of South Greenland late-glacial ice limits from a new relative sea level curve. *Earth Planet. Sci. Lett.* **197,** 171–186 (2002).
86. Zwartz D., Bird, M., Stone, J. & Lambeck, K. Holocene sea-level change and ice-sheet history in the Vestfolf Hills, East Antarctica. *Earth Planet. Sci. Lett.* **155,** 131–145 (1998).
87. CLIMAP Project Members. The surface of the ice age Earth. *Science* **191,** 1131–1137 (1976).
88. Lambeck, K., Yokoyama, Y., Johnston, P. & Purcell, A. Global ice volumes at the Last Glacial Maximum and early Late glacial. *Earth Planet. Sci. Lett.* **181,** 513–527 (2000).
89. Elliot, M. *et al.* Millennial-scale iceberg discharges in the Irminger Basin during the last glacial period: relationship with the Heinrich events and environmental settings. *Paleoceanography* **13,** 433–446 (1998).
90. Shemesh, A., Burckle, L. H. & Hays, J. D. Meltwater input to the Southern Ocean during the Last Glacial Maximum. *Science* **266,** 1542–1544 (1994).
91. Petit, J. R. *et al.* Climate and atmospheric history of the past 420,000 years from the Vostok ice core, Antarctica. *Nature* **399,** 429–436 (1999).

92. Stoffers, P. & Ross, D. A. Late Pleistocene and Holocene sedimentation in the Persian Gulf-Gulf of Oman. *Sedim. Geol.* **23,** 181–208 (1979).
93. Fairbanks, R. G. A 17,000-year glacio-eustatic sea level record: influence of glacial melting rates on the Younger Dryas event and deep-ocean circulation. *Nature* **342,** 637–642 (1989).
94. Bard, E., Hamelin, B. & Fairbanks, R. G. U-Th ages obtained by mass spectrometry in corals from Barbados: sea level during the past 130,000 years. *Nature* **346,** 456–458 (1990).
95. Bard, E. *et al.* Deglacial sea-level record from Tahiti corals and the timing of global meltwater discharge. *Nature* **382,** 241–244 (1996).
96. Hanebuth, T., Stattegger, K. & Grootes, P. M. Rapid flooding of the Sunda Shelf: a late-glacial sea-level record. *Science* **288,** 1033–1035 (2000).
97. Clark, P. U. *et al.* Origin of the first global meltwater pulse following the last glacial maximum. *Paleoceanography* **11,** 563–577 (1996).
98. Clark, P. U., Mitrovica, J. X., Milne, G. A. & Tamisiea, M. E. Sea-level fingerprinting as a direct test for the source of global meltwater pulse IA. *Science* **295,** 2438–2441 (2002).
99. Johnson, R. G. Major northern hemisphere deglaciation caused by a moisture deficit 140 ka. *Geology* **19,** 686–689 (1991).
100. Shaffer, J. A., Cerveny, R. S. & Dom, R. I. Radiation windows as indicators of an astronomical influence on the Devil's Hole chronology. *Geology* **24,** 1017–1020 (1996).

Acknowledgements

This research was supported by the Australian National University and by the Swedish Research Council. We thank S. Björck for constructive comments and M. E. Raymo and G. H. Haug for providing the data sets for Fig. 1.